Journal of Advanced Research in Applied Sciences and Engineering Technology

Journal homepage:
https://semarakilmu.com.my/journals/index.php/applied_sciences_eng_tech/index
ISSN: 2462-1943

Optimum Performance Achieving of BLDC Motor Based on Optimized SMC Strategy

Ahmed Maher Kheel[1,*], Nabil Kadhim Al-Shamaa[1], Majli Nema Hawas[2]

[1] Department of Electrical Power Engineering Techniques, Electrical Engineering Technical College, Middle Technical University, Baghdad, Iraq
[2] Institute of Technology Baghdad, Middle Technical University, Al-Za'franiya, 10074 Baghdad, Iraq

ARTICLE INFO

Keywords:
Particle swarm optimization (PSO); Proportional-integral (PI); Sliding mode controller (SMC); speed control of BLDC motor

ABSTRACT

Electric vehicles, healthcare devices, and manufacturing machinery all use brushless DC motors (BLDCM) because of the need for precise speed regulation to accommodate load and reference variation. In this research, the Particle Swarm Optimization (PSO) method is used to find the best values for the Proportional-Integral (PI) and Sliding Mode Controller (SMC) parameters used to regulate the speed of BLDC motors. The Integral Time Absolute Error (ITAE) is employed as the fitness function when utilizing the PSO technique for fine-tuning the PI and SMC parameters. Statistical and visual representations of the optimization techniques' effectiveness are provided. The simulation results demonstrate the PSO-based SMC's superiority over the optimization PI controller and the SMC without optimization regarding fast-tracking to the intended value and reduced torque ripple under non-uniform situations.

1. Introduction

In light of recent advances in power electronics, control theory, and permanent magnetic materials, BLDCM designed a novel DC motor. For numerous reasons, it quickly replaced the conventional motor in applications as diverse as precision electronic machinery, robotics, airplanes, chemical mining, and many others [1,2]. Many types of electric motors have been proposed for this use [1]. Standard DC motors, for example, are known for their exceptional performance. On the other hand, traditional DC motors have a few limitations that make them less than ideal. Regular brush replacement and the usage of commutators are necessities. Put in at the start [3-6], and traditional DC motors cannot be used where dust or explosions could be a problem. One variety of induction motors is the squirrel-cage design. Durable enough to serve as a replacement for the typical DC motor. Despite its low cost, it has several drawbacks [1,7-9] that make it less than ideal. In addition, conventional DC motors and induction motors are both wrong choices. In high-speed applications, the DC brushless motor—a hybrid of a DC motor and an induction motor—is often referred to as direct current (DC) or alternating current (AC) power. Commutation is performed via solid-state

* *Corresponding author.*
E-mail address: bcc0051@mtu.edu.iq

https://doi.org/10.37934/araset.64.2.149164

switches. Rotor position and location are sent to establish time. The rotor's speed or function can be detected using position sensors or sensor less methods. The stability of the BLDCM must be maintained under changing loads and parameters using a control strategy that is flexible, robust, accurate, and simple to implement [1,7-11]. The PID controller has many applications [1] because of its versatility, robustness, dependability, and ease of parameter modification. Although the Ziegler-Nichols rule is commonly used to determine PID parameters, it is not the optimal choice in all cases. It is possible to utilize a genetic optimization method using three different cost functions to get the best settings for the PID controller. Rapid changes in set point and parameter variation are the most difficult situations for PID control to adapt to [4]. This problem can be tackled with the help of state-of-the-art control methods such as adaptive control, variable structure control, fuzzy control, and neural networks [4,9,10].

One of the main challenges with applying self-tuning adaptive control systems is the inability to perform trajectory control in the event of unexpected disturbances or large sounds. The parameter estimator may give erroneous results [6] in the face of sudden disturbances or deafening noises. The variable structure controller is easy to understand in theory but difficult to implement in practice. This is because a change in the control signal could cause system problems if executed suddenly [9]. However, additional processing power and storage space are needed for a neural network-based motor control system to handle system-level structure uncertainty and disturbance effectively [4]. Even for nonlinear systems, nonlinear controllers grounded in fuzzy control theory are often capable of performing a wide range of nonlinear control actions [4-10]. Unlike conventional control design, an FLC does not require precise knowledge of the system model, such as the poles and zeroes of the system transfer function [11].

An expert understanding of a database-based fuzzy logic control system may need fewer calculations but cannot accommodate the new rules [7,11,12]. Sliding mode control (SMC) is employed for these problems [13]. Maintaining system stability using SMC is possible in several models with various interference and system parameters. As a result of this, it is utilized extensively in nonlinear models. Because it has a working area in the steady state phase, SMC can effectively maintain system performance despite parameter disruptions and changes. We can position the SMC sliding surface in the most advantageous location thanks to cutting-edge technology known as SMC, which is based on an optimization algorithm. It is possible to improve the system's transient response using this SMC instead of the previous one [14,15]. Particle Swarm Optimization (PSO) [16], Moth Swarm Algorithm (MSA) [17], Bat Algorithm [18], and bacterial Foraging Algorithm [19] are some of the artificial intelligence algorithms that numerous authors have increasingly added to the standard PID control in recent years.

To the best of the authors' knowledge, this article marks the first time that a novel algorithm, called Particle Swarm Optimization (PSO), has been utilized to tune the parameters of SMC for speed control of BLDCM. An outer and an inner closed loop are essential to the proposed control strategy. The inner loop regulates the current, while the outer loop regulates the speed. The suggested regulation is easy to implement and reliable. In recent advancements in magnetic field analysis and motor control technology, several innovative methods have been explored to enhance the precision and reliability of BLDC motor speed control. In 2021, the focus was primarily on Magnetic Field Analysis, which involved extracting precise measurements from noise in magnetic fields, a critical factor in enhancing the reliability and efficiency of motor control systems [20].

By 2023, research has broadened into optimizing controller techniques for BLDC motors. The Fractional-Order PID Controller (FOPID), utilizing Nelder-Mead Optimization, is a notable development, offering an optimized circuit implementation for refining BLDC motor speed control, making significant strides in ensuring smoother and more responsive motor operation [21].

Concurrently, introducing the Chaotic Adaptive Tuning Strategy (CATSCG) signifies another innovative approach, where the adaptive tuning of controller gains has been applied to regulate the speed of BLDC motors proficiently [22]. Developing the Higher-Order Sliding Mode Controller (HOSMC) also underscores a robust method for BLDC motor speed control, providing a resilient solution to system uncertainties and external disturbances [23]. These evolving methodologies underscore a sustained effort in refining motor control mechanisms, emphasizing precision, adaptability, and robustness in diverse operational conditions.

2. Modeling of BLDC Motor

The mathematical model is necessary for analyzing the dynamic response and studying the behavior of the BLDC motor. The corresponding circuit of a BLD motor is depicted in Figure 1. Eq. (1) [1, 2] deduces the differential voltage equations regarding the equivalent circuit.

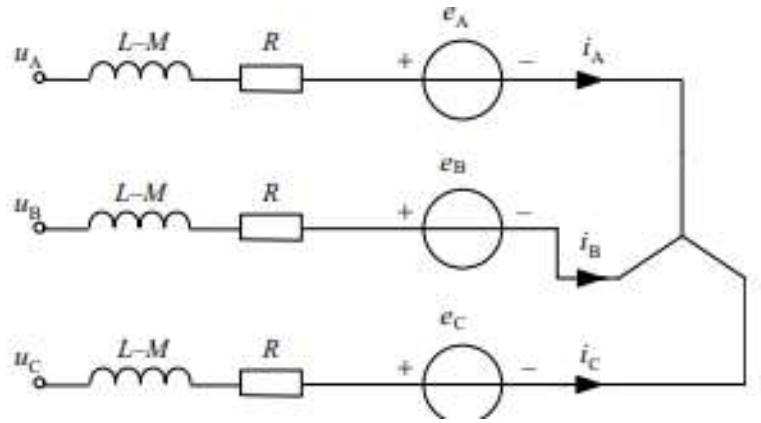

Fig. 1. The BLDC motor's equivalent circuit

$$\left.\begin{aligned} v_a &= R_a i_a + L_a \frac{di_a}{dt} + L_{ab}\frac{di_b}{dt} + L_{ca}\frac{di_c}{dt} + e_a \\ v_b &= R_b i_b + L_b \frac{di_b}{dt} + L_{ba}\frac{di_a}{dt} + L_{bc}\frac{di_c}{dt} + e_b \\ v_c &= R_c i_c + L_a \frac{di_a}{dt} + L_{ab}\frac{di_b}{dt} + L_{ca}\frac{di_c}{dt} + e_c \end{aligned}\right\} \tag{1}$$

Eq. (1) might also have been written as a matrix:

$$\begin{bmatrix} v_a \\ v_b \\ v_c \end{bmatrix} = \begin{bmatrix} R_a & 0 & 0 \\ 0 & R_b & 0 \\ 0 & 0 & R_c \end{bmatrix} \begin{bmatrix} i_a \\ i_b \\ i_c \end{bmatrix} + \frac{d}{dt} \begin{bmatrix} L_a & L_{ab} & L_{ca} \\ L_{ba} & L_b & L_{bc} \\ L_{ca} & L_{cb} & L_c \end{bmatrix} \begin{bmatrix} i_a \\ i_b \\ i_c \end{bmatrix} + \begin{bmatrix} e_a \\ e_b \\ e_c \end{bmatrix} \tag{2}$$

Most BLDC motors have a salient-pole rotor positioned on the motor's outside. In this case, the time does not affect the inductance of the windings. In addition, the self-inductances and mutual inductances will be equivalent in a three-phase stator with symmetric windings. Thus, we have:

$$i_a + i_b + i_c = 0 \tag{3}$$

$$L_a = L_b = L_c = L_s \tag{4}$$

$$R_a = R_c = R_c = R \tag{5}$$

$$L_{ab} = L_{ac} = L_{bc} = L_{ba} = L_{ca} = L_{ab} = M \tag{6}$$

Since Eq. (2) can be rewritten as:

$$\begin{bmatrix} v_a \\ v_b \\ v_c \end{bmatrix} = \begin{bmatrix} R & 0 & 0 \\ 0 & R & 0 \\ 0 & 0 & R \end{bmatrix} \begin{bmatrix} i_a \\ i_b \\ i_c \end{bmatrix} + \frac{d}{dt} \begin{bmatrix} L_s & M & M \\ M & L_s & M \\ M & M & L_s \end{bmatrix} \begin{bmatrix} i_a \\ i_b \\ i_c \end{bmatrix} + \begin{bmatrix} e_a \\ e_b \\ e_c \end{bmatrix} \tag{7}$$

where $\mathrm{L} = L_s - M$, and the phase voltage equations of a BLDC motor can thus be represented in matrix form as:

$$\begin{bmatrix} v_a \\ v_b \\ v_c \end{bmatrix} = \begin{bmatrix} R & 0 & 0 \\ 0 & R & 0 \\ 0 & 0 & R \end{bmatrix} \begin{bmatrix} i_a \\ i_b \\ i_c \end{bmatrix} + \frac{d}{dt} \begin{bmatrix} L & M & M \\ M & L & M \\ M & M & L \end{bmatrix} \begin{bmatrix} i_a \\ i_b \\ i_c \end{bmatrix} + \begin{bmatrix} e_a \\ e_b \\ e_c \end{bmatrix} \tag{8}$$

The equations for the trapezoidal back EMF can be stated as follows:

$$\left.\begin{aligned} e_a &= K_e \omega_r F(\theta_e) \\ e_a &= K_e \omega_r F\left(\theta_e - \frac{2\pi}{3}\right) \\ e_a &= K_e \omega_r F\left(\theta_e + \frac{2\pi}{3}\right) \end{aligned}\right\} \tag{9}$$

In conclusion, the Equation for the torque that was developed can be represented as follows:

$$T_e = K_\omega \omega_r F(\theta_e) i_a + K_\omega \omega_r F\left(\theta_e - \frac{2\pi}{3}\right) i_b + K_\omega \omega_r F\left(\theta_e + \frac{2\pi}{3}\right) i_c \tag{10}$$

Alternately, it can be portrayed following the motion equation, and in this case, we have:

$$T_e = J \frac{d\omega_r}{dt} + B\omega_r + T_l \tag{11}$$

The definition of the function F could be as follows:

$$F(\theta_e) = \left.\begin{aligned} & 1 \; if \; 0 \le \theta_e < \frac{2\pi}{3} \\ & 1 - \frac{6}{\pi}\left(\theta_e - \frac{2\pi}{3}\right) if \; \frac{2\pi}{3} \le \theta_e < \pi \\ & -1 \; if \; \pi \le \theta_e < \frac{5\pi}{3} \\ & -1 + \frac{6}{\pi}\left(\theta_e - \frac{5\pi}{3}\right) \; if \; \frac{5\pi}{3} \le \theta_e < 2\pi \end{aligned}\right\} \tag{12}$$

3. Results Control Strategy

In this work, comparing the optimization of PI controllers and SMC controllers was the primary topic. In order to facilitate a fruitful comparison, the concepts of PI and SMC are modeled and explained in the following sections.

3.1 PI Controller

PI control is frequently utilized in industrial control systems. This is primarily because parameter adjustments can be made concerning the output characteristics of the system. The PI controller can be described using the general equation as follows:

$$u(t) = K_p e(t) + K_i \int e(t)dt \tag{13}$$

where $e(t) = \omega_r{}^* - \omega_r$.

An overshoot will be observed at the output when the controller parameters are adjusted to inappropriately high levels. On the other hand, when the parameter magnitudes are small, it can take a long time to reach the reference speed, or there might be an inaccuracy in the steady state. Because of this, the optimization technique is required to alter the optimal settings of the PI controller to get a higher level of performance for any system being investigated.

3.2 SMC Controller

The formation of the sliding surface is the initial step in the design process for the SMC. The Equation that is typically employed for describing the sliding surface can be expressed as follows, in general:

$$\mathrm{s(t)} = C\,X_1 + X_2 = \mathrm{C\,e(t)} + \dot{e}(t) \tag{14}$$

$$\dot{s}(t) = C\,\dot{X_1} + \dot{X_2} = C\,\dot{e}(t) + \ddot{e}(t \tag{15}$$

where $e(t) = y^* - y$.

It has been demonstrated that sliding surface is an action associated with tracking error, defined as any difference between the reference and actual output in this area. The system's stability could be guaranteed if C was more significant than 0. This is a performance parameter. On a surface that allows sliding [4, 11, 23] the sliding function and its derivative are equal to zero throughout the sliding surface, so $s(t)$ 0 and $s(t)$ = 0 are equivalent to zero. The control signal law u(t) is the objective of the SMC and consists of two elements, which are inferred in Eqs. (16), (17) and (18). The equivalent control signal $u_{eq}(t)$ and the switching control signal $u_{sw}(t)$.

$$u(t) = u_{eq}(t) + u_{sw}(t) \tag{16}$$

$$u_{sw}(t) = k\,sgn(s) \tag{17}$$

where:

$$Sgn\left(s(t)\right) = \begin{cases} +1, if\ s\ (t) > 0 \\ 0, if\ s\ (t) = 0 \\ -1. If\ s\ (t) < 0 \end{cases} \tag{18}$$

$sgn(\cdot)$ is referred to as the signum function, and it is defined as follows: where k is a positive design parameter. It is chosen to be quite large to suppress the system's uncertainties, and unexpected dynamic $s(t)$ is less than zero. The signal $u_{sw}(t)$ pulls the system states toward the sliding surface. When the sliding surface has been reached, the switching control signal will no longer be active. Even if the equivalent control signal is continuous, the switching control signal is discontinuous [7, 24-26]. This is because of the scenario.

It is possible to rewrite the motion equation that is described in Eq. (11) as follows:

$$J\frac{d\omega_r}{dt} = k_t u - B\omega_r - T_l \tag{19}$$

In terms of the possible errors, the sliding surface can be stated as:

$$s\ (\omega) = Ce - \dot{e} \tag{20}$$

In cases in which the tracking error is equal to: $e(t) = \omega_r{}^* - \omega_r$.

Assume the $s(\dot{\omega}) = 0$, and we have:

$$s\ (\dot{\omega}) = e = \dot{\omega_r}^* - \dot{\omega_r} = \dot{\omega_r}^* - \frac{k_t}{J}u + \frac{B}{J}\omega + \frac{1}{J}T_l = 0 \tag{21}$$

The comparable control was developed following the observer torque, and its representation may be seen as:

$$u_{eq} = \frac{1}{k_t}(J\dot{\omega_r}^* + B\omega + T_l) \tag{22}$$

In addition, the switching control is dependent on the signal from the sliding surface, which can be formulated as follows:

$$u_{sw} = k\ sgn(s) \tag{23}$$

In conclusion, the actual control is being produced due to the addition of the switch control and the equivalent control rule.

$$u = u_{eq} + u_{sw} \tag{24}$$

The final version of the actual control equation that depends on simulation can be obtained by substituting Eqs. (22) and (23) into Eq. (24). This results in the following:

$$u = \frac{1}{k_t}(J\dot{\omega_r}^* + B\omega + T_l) + k\ sgn(s) \tag{25}$$

Eq. (25) is utilized in the process of regulating the output speed of BLDC motors in order to achieve the desired speed under a variety of different conditions.

4. Proposed Control Structure

Figure 2 illustrates the proposed control method, which consists of two control loops: a speed control loop and a current control loop. Both of these loops can be controlled independently of one another SMC is employed as a speed controller in this work. A comparison is made with the PI controller to demonstrate which method is more effective in following the desired trajectory. However, the PI controller is utilized to manage the stator current of the BLDCM. In order to obtain outstanding performance in non-uniform situations, the PSO algorithm is used to tune the controller parameters for a pair of PI controllers.

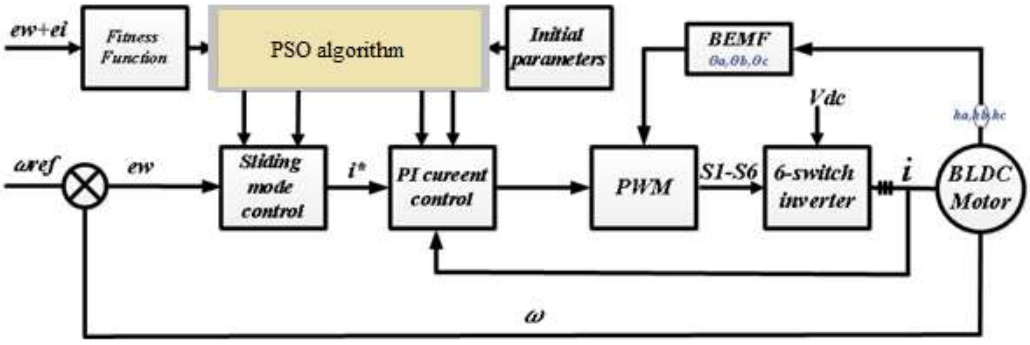

Fig.2. Suggested control strategy of BLDC motor

5. Particle Swarm Optimization (PSO)

The Particle Swarm Optimization (PSO) algorithm is a stochastic optimization algorithm inspired by the social behaviour of bird flocks and fish schools. The algorithm involves a population of particles that move around in the search space to find the optimal solution to a given problem. The PSO algorithm is defined by the following equations:

i. Initialization: The algorithm starts by initializing a population of N particles, each with a position and a velocity vector. The position vector represents a candidate solution to the problem, while the velocity vector determines the direction and speed of the particle's movement in the search space.
ii. Evaluation: The fitness of each particle's position is evaluated based on the objective function of the problem. The objective function usually measures how well the candidate solution satisfies the problem constraints and requirements [27].
iii. Updating the particle's velocity: The velocity of each particle is updated using the following equation:

$$v_i(t+1) = wv_i(t) + c1r1 * (pbest_i - x_i(t)) + c2r2(gbest - x_i(t)) \quad (26)$$

where $v_i(t)$ is the velocity of the ith particle at time t. w is the inertia weight that controls the balance between the particle's previous velocity and the social and cognitive components. $c1$ and $c2$ are the acceleration coefficients controlling the impact of the particle's personal and global best positions on its velocity. $r1$ and $r2$ are random numbers between 0 and 1 that introduce stochasticity to the algorithm. $pbest_i$ is the personal best position of the ith particle, which is the position with

the best fitness that the particle has found so far. $x_i(t)$ is the current position of the ith particle at time t. $gbest$ is the global best position of all particles, which is the position with the best fitness among all particles in the population.

iv. Updating the particle's position: The position of each particle is updated using the following equation:

$$x_i(t+1) = x_i(t) + v_i(t+1) \tag{27}$$

where $x_i(t)$ is the current position of the ith particle at time t, and $v_i(t+1)$ is the updated velocity of the particle at time $t+1$.

v. Updating the personal and global best positions: The personal best position of each particle is updated if its fitness improves, and the global best position is updated if any particle finds a better solution than the current global best.

vi. Termination: The algorithm terminates when a stopping criterion is met, such as a maximum number of iterations or a satisfactory level of fitness for the best solution found.

6. Simulation Results

This section compares the performance of the proposed SMC controller in non-uniform conditions to that of an optimizer PI controller that uses the PSO algorithm and has the same restrictions (search agent = 10 and maximum iteration = 50). Table 1 contains a listing of the BLDC motor model parameters that were utilized in the simulations. The optimal controller parameters have been calculated using the PSO method and are presented in Table 2. The tracking performance of the fitness function when using a PSO-based SMC and PI controller is shown in Figure 3. This figure makes it abundantly clear that the SMC with PSO technique is less effective in fitness than the PI with PSO strategy. The dynamic response underrated settings (w = 4000 RPM and load torque is changed from 0.16 to 0.32 Nm) and the emotional reaction under non-uniform conditions are separately investigated in the simulation results to demonstrate the superiority of the proposed system. w = 4000 rpm, and load torque is changed from 0.16 to 0.32 Nm.

Table 1 provides specifications for the discussed system, including parameters such as DC voltage (Vdc), rated torque (Te), rated speed (ω), inductance (L), resistance (R), maximum current (Ia), number of poles (P), torque constant (Kt), and moment of inertia (J). These values are essential for understanding the system's performance and design characteristics.

Table 2 presents the parameters of the proposed controllers, including Sliding Mode Controller (SMC), Speed Controller, and Current Controller. These parameters are derived using Ziegler-Nichols and Particle Swarm Optimization (PSO) techniques. Table 2 displays specific values for proportional (Kp) and integral (Ki) gains for each controller, providing essential information for the study.

6.1 Case I: Simulation Results of BLDC Motor Underrated Speed and Variable Load

As shown in Figures 4-8, the optimization SMC generally has a much quicker response time than the optimization PI control. In Figure 4, we can see that the SMC- and PSO-SMC-based speed responses are superior due to their minor steady-state errors and overshoots compared to the PI- and PSO-PI-based speed responses.

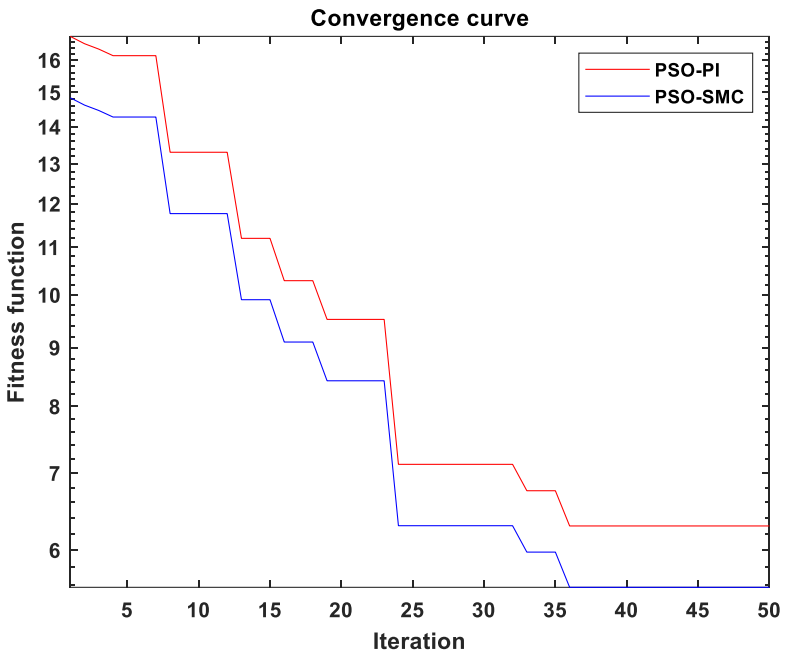

Fig. 3. The objective function of SMC and PI is based on the PSO algorithm

Table 1
Specifications

Parameters	Value	Unit
DC voltage	Vdc	36 V
Rated torque	Te	0.32 Nm
Rated speed	ω	4000 rpm
Inductance	L	1.4 mH
maximum current	Ia	16.5 A
Resistance	R	0.45 Ω
maximum current	Ia	6 A
Number of poles	P	4
Torque constant	Kt	0.063 Nm/A
Number of poles	P	4
Moment inertia	J	0.0000173 Kg/m^2

Table 2
Parameters of the proposed controllers

Techniques	SMC		Speed controller		Current controller	
	C	K	Kp	Ki	Kp	Ki
Ziegler-Nichols	1800	4500	7.8	18	8	0.88
PSO	1066.334	3452.457	0.704	11.457	88.47	58.147

Figure 5 shows that the SMC and PSO-SMC did a better job of removing overshoot and torque ripple than the PI and optimal PI controllers and that the PSO-SMC produces less chattering.

Although the velocity error for all four approaches is shown in Figure 6, the PSO with SMC achieves the best results in minimizing the error and keeping the velocity constant.

Figure 7 displays underestimated stator current settings, highlighting the need for precise current control. PSO-SMC corrects these discrepancies, optimizing system efficiency.

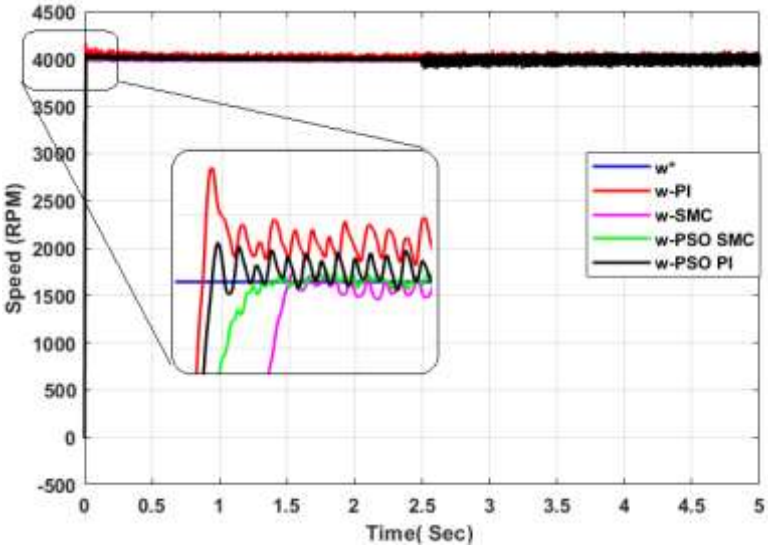

Fig. 4. Performance of BLDCM speed

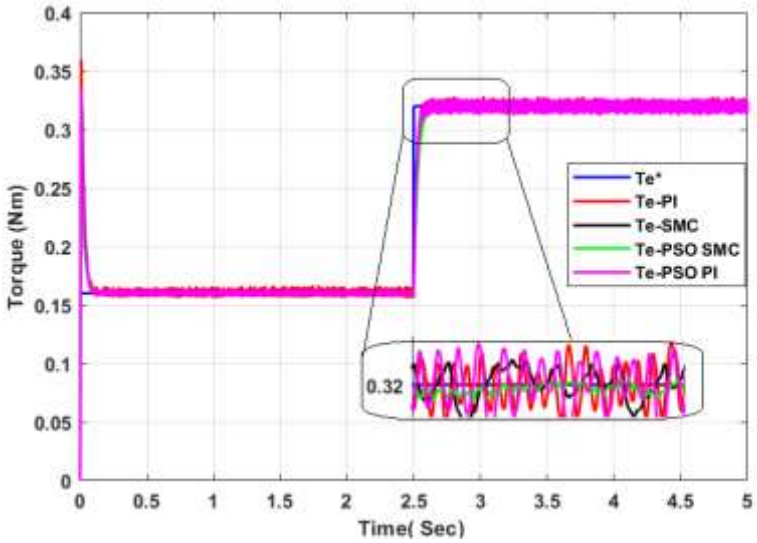

Fig. 5. Comparison performance of torque behaviour of BLDCM

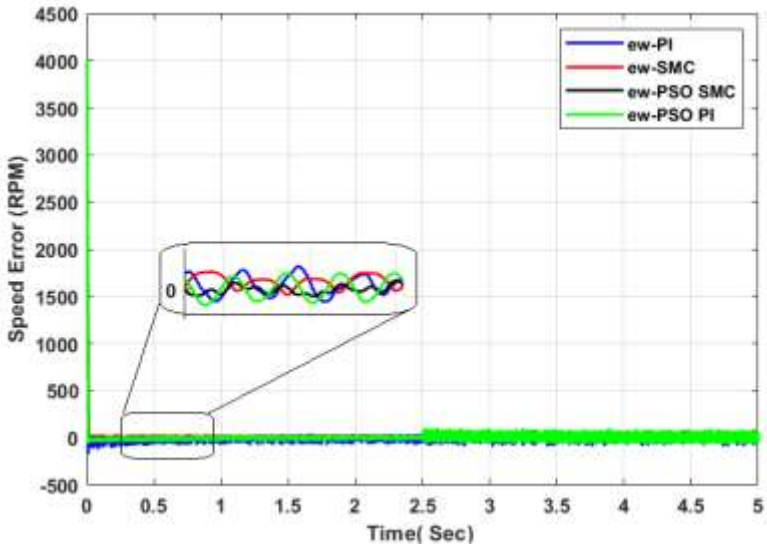

Fig. 6. Comparison of speed error

Figure 8 illustrates the underestimated settings for the trapezoidal back EMF voltage. The deviations observed here emphasize the impact of inaccurate back EMF voltage estimation on system behavior. Optimal back EMF voltage is essential for achieving efficient motor operation. In the context of PSO-SMC, this figure underscores the algorithm's effectiveness in rectifying these inaccuracies. By identifying and correcting these voltage discrepancies, PSO-SMC ensures that the motor operates at its optimal back EMF voltage, leading to enhanced performance and stability. These results underscore the critical role of PSO-SMC in achieving precise back EMF voltage control, crucial for the overall effectiveness of the motor control system.

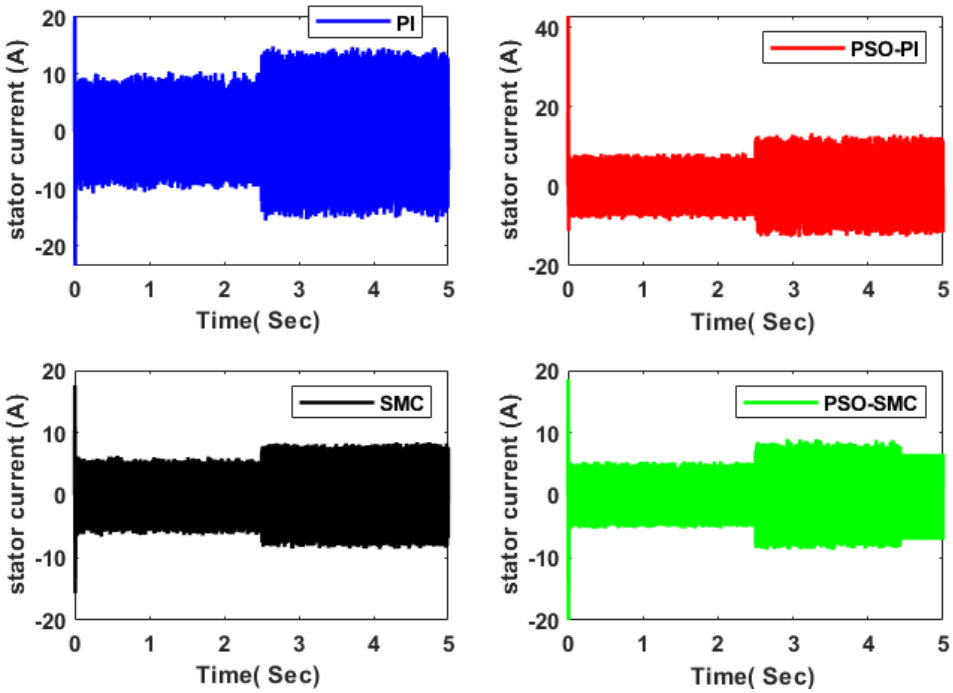

Fig. 7. State stator currents response of BLDCM

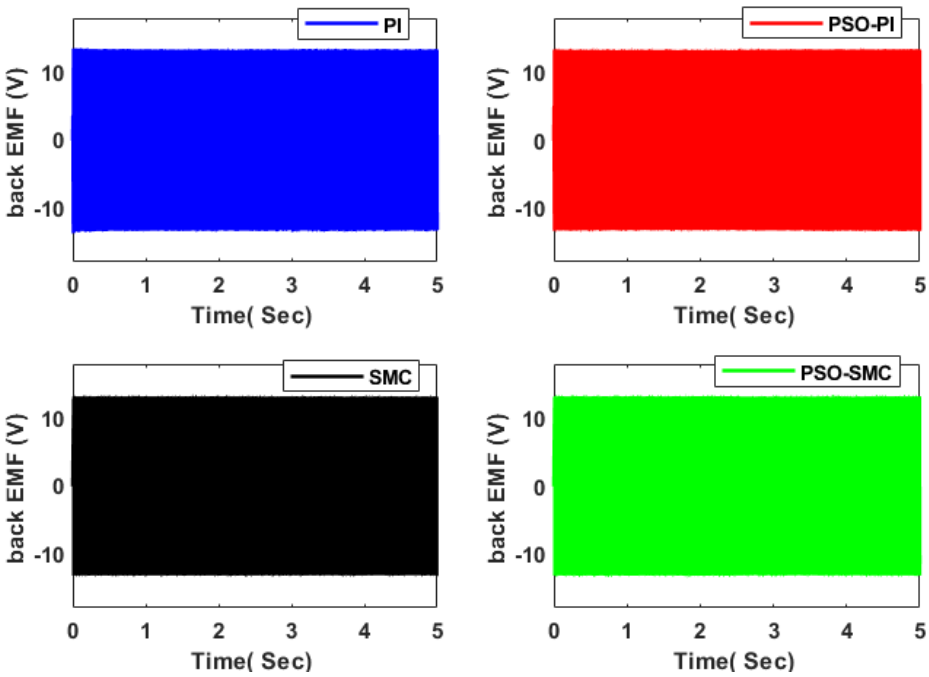

Fig. 8. Back EMF behaviour of BLDCM

6.2 Case II: Simulation Results of BLDC Motor Under Random Speed and Constant Load

The proposed system is tested at varying speeds under a constant load of 0.32 Nm to demonstrate the robustness of the proposed control strategy when used in conjunction with the PSO algorithm. Looking at Figure 9 makes it clear that the speed response was established. Under variable speed conditions, PSO-SMC's speed response is characterized by rapid convergence to the desired value and accurate trajectory tracking with no overshoot and very little chattering. The standard method of SMC has been upgraded.

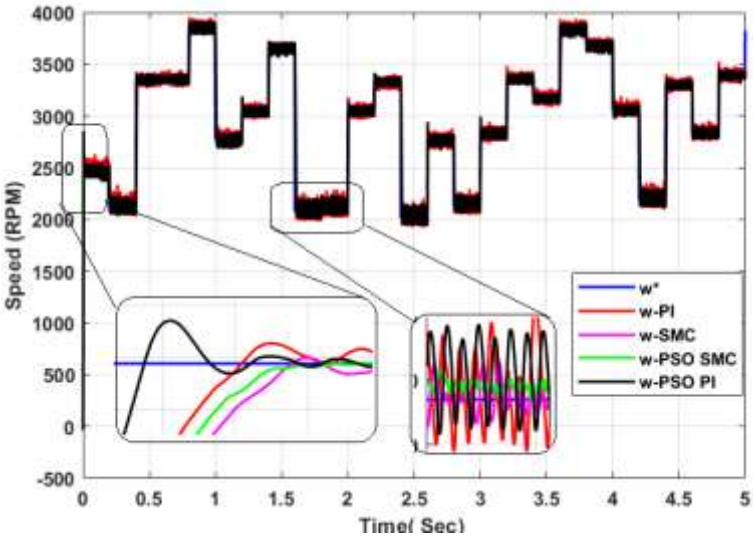

Fig. 9. Speed dynamic response of BLDCM

Figure 10 illustrates the dynamic torque behavior of the Brushless DC Motor (BLDCM) under the PSO-SMC controller. The graph showcases how the controller optimally fast-tracks the motor to the target trajectory.

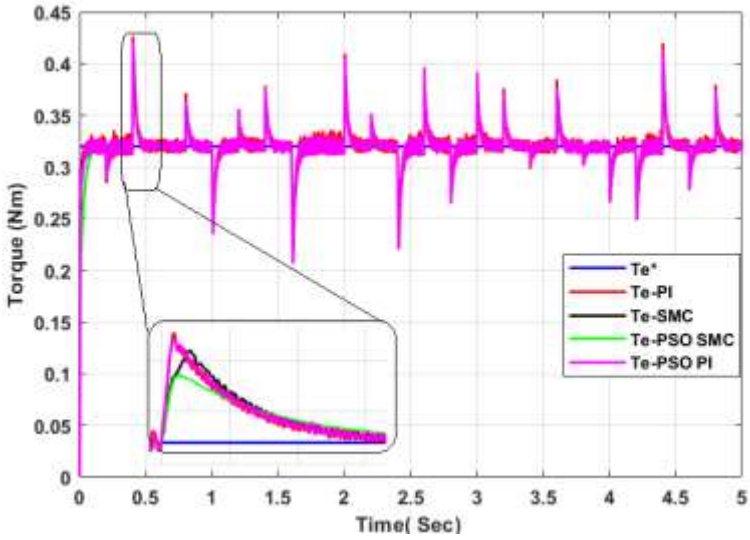

Fig. 10. Dynamic torque behaviour of BLDCM

Figure 11 displays the speed rotor error achieved through the PSO-SMC controller. The graph highlights the minimal deviation between the desired speed and the actual rotor speed.

In Figure 12, the stator currents exhibit rapid adjustments in response to random speed changes. The graph illustrates the immediate shifts in stator current, showing how the system swiftly adapts to varying speeds. This response, as depicted in the figure, highlights the system's ability to quickly reach equilibrium without experiencing overshoot. Such behavior is crucial for stable and efficient operation in dynamic conditions.

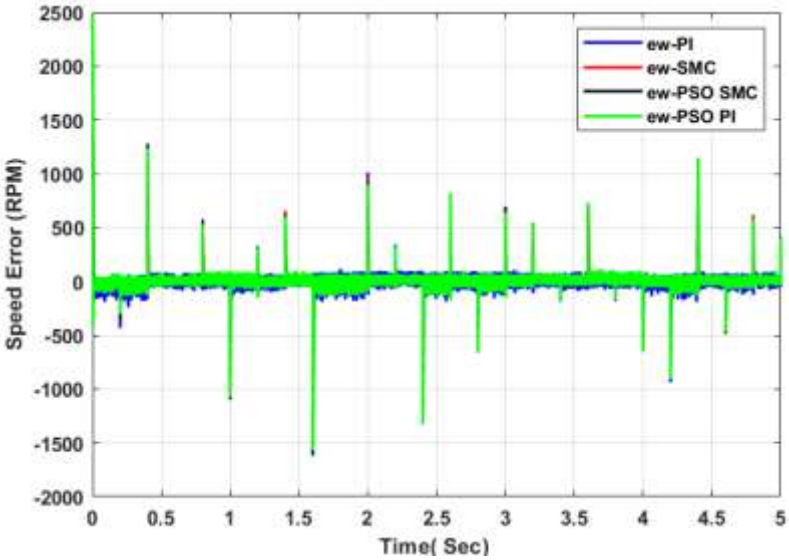

Fig.11. Speed rotor error

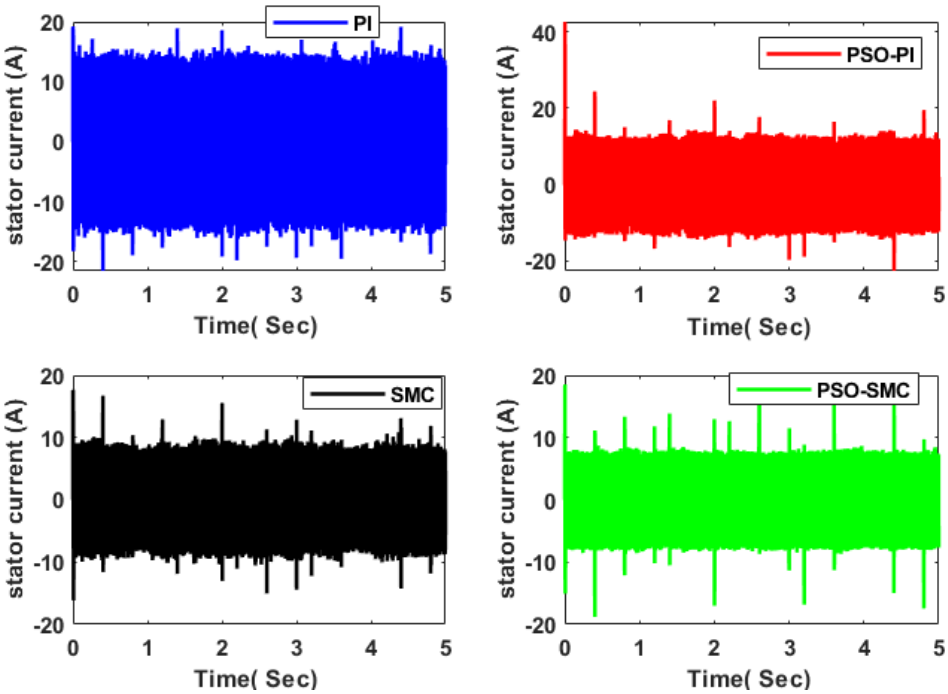

Fig.12. Response of stator currents under random speed applied

Figure 13 portrays the dynamic response of the back electromotive force (EMF) under random operating conditions. The graph demonstrates how changes in speed and torque prompt instantaneous shifts in the back EMF voltage.

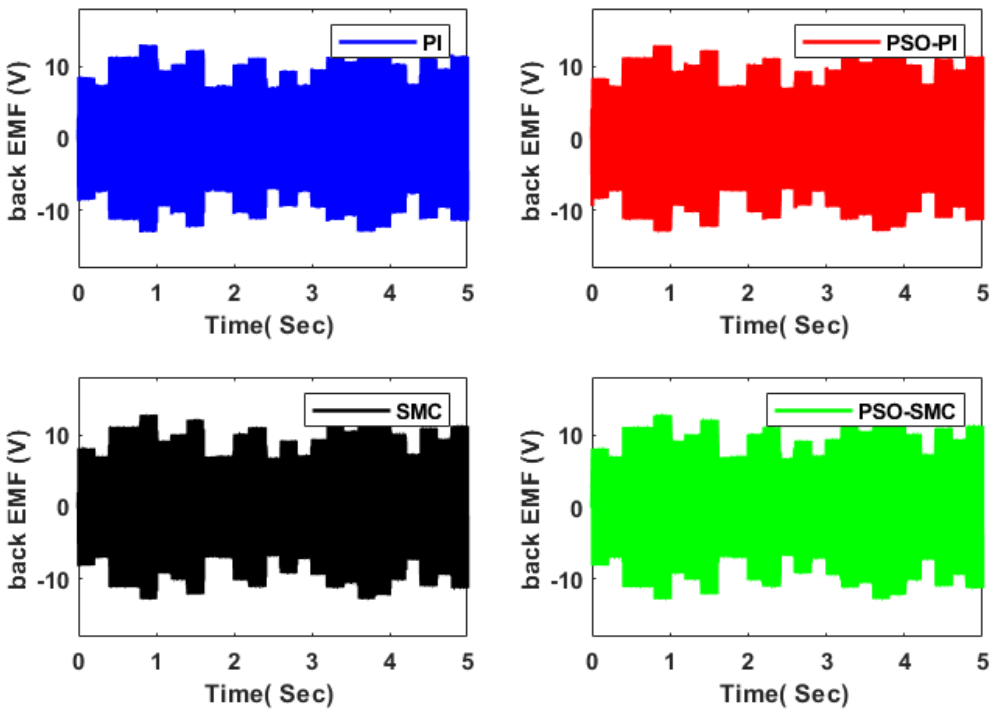

Fig. 13. Dynamic back EMF response under random conditions

Table 3 shows the specifications for evaluating the proposed SMC based on the PSO algorithm and another conventional method. The purpose of this analogy is to clarify the situation. Table 3 shows that the PSO-SMC reaches a steady state more quickly due to its shorter rise and settling times. In addition, its steady-state performance is excellent, with no overshoot and minimal ripple.

Table 3
Performance of SMC and PI controllers

Technique	ITAE	Overshoot (RPM)	Rise time	Settling time	Ripple (RPM)
PSO-PI	6.2967	68	18.45ms	24ms	± 57.4
PSO-SMC	4.5390	0	5.5ms	7.2ms	±7.52

7. Conclusions

The parameters of the PI controller and the sliding mode controller are optimized using the PSO algorithm in this study. Here, we opt to control the rotational speed of the BLDC motor. The ITAE is a fitness function based on the summation errors of comparisons between actual speed and reference speed to decrease torque ripple in BLDC motors and achieve excellent tracking for rate under varying conditions. The results of the simulations show that BLDC motors perform similarly to optimized PI and conventional SMC regardless of the speed and load torque variations. Future research could benefit from developing optimization algorithms for BLDC motor speed control, considering a more comprehensive range of system parameters. In our exploration of BLDC motor optimization, the standout strength is the meticulous integration of derivative components for refined predictive control. The fusion of adaptive strategies and cutting-edge optimization accentuates our commitment to mitigating overshoot through optimal parameter identification amidst intricate dynamics and nonlinearities. Incorporating feedforward elements and implementing Model Predictive Control (MPC) underline our endeavour for holistic optimization and proactive disturbance counteraction in scientific forums.

Acknowledgement
Authors would like to express our gratitude to the Electrical Engineering Technical College as well as every member of the teaching team for all their help. This research was not funded by any grant.

References
[1] Xia, C.-l. (2012). *Permanent Magnet Brushless Dc Motor Drives and Controls.* John Wiley & Sons.
[2] El Idrissi, A.L., Jamal B., M.M., and Anas B. "Comparative Study between Pi Speed Control and Sliding Mode Control of Bldc Motor." *Advances in Smart Technologies Applications and Case Studies* (2020): 309-317. https://doi.org/10.1007/978-3-030-53187-4_35
[3] Yuanxi, W., Yu Y., Zhang G., and Sheng X. "Fuzzy Auto-Adjust Pid Controller Design of Brushless Dc Motor." *Physics Procedia* 33, (2012): 1533-1539. https://doi.org/10.016/j.phpro.2012.05.249
[4] Orman, K. "Design of a Memristor-Based Chattering Free Sliding Mode Controller and Speed Control of the Bldc Motor." *Tehnički vjesnik* 28, no. 3 (2021): 754-62. https://doi.org/10.17559/TV-20200105141443
[5] Siong, T.C., Baharuddin I., Siti F.S., Mohd F.N.T., Noor S.J., and Mohd F.M. "Analysis of Fuzzy Logic Controller for Permanent Magnet Brushless Dc Motor Drives." *2010 IEEE Student Conference on Research and Development (SCOReD)* (2010): 436-441. https://doi.org/10.1109/SCORED.2010.5704049
[6] Shamseldin, M.A., and EL-Samahy, A.A. "Speed Control of Bldc Motor by Using Pid Control and Self-Tuning Fuzzy Pid Controller." *15th International Workshop on Research and Education in Mechatronics (REM)* (2014): 1-9. https://doi.org/10.1109/REM.2014.6920443
[7] Shao, Y., Rongrong Y., Jianwen G., and Yongling F. "Sliding Mode Speed Control for Brushless Dc Motor Based on Sliding Mode Torque Observer." *2015 IEEE International Conference on Information and Automation* (2015): 2466-2470. https://doi.org/10.1109/ICInfA.2015.7279700
[8] Sankar, A.B., and Seyezhai, R. "Simulation and Implementation of Sensored Control of Three-Phase Bldc Motor Using Fpga." *2014 International Conference on Science Engineering and Management Research (ICSEMR)* (2014): 1-5. https://doi.org/10.1109/ICSEMR.2014.7043619
[9] Premkumar, K., and Manikandan B. V. "Speed Control of Brushless Dc Motor Using Bat Algorithm Optimized Adaptive Neuro-Fuzzy Inference System." *Applied Soft Computing* 32, (2015): 403-419. https://doi.org/10.1016/j.asoc.2015.04.014
[10] Premkumar, K., and Manikandan, B.V. "Fuzzy Pid Supervised Online Anfis Based Speed Controller for Brushless Dc Motor." *Neurocomputing* 157, (2015): 76-90. https://doi.org/10.1016/j.neucom.2015.01.032
[11] Prasad, K.M.A., and Nair, U. "An Intelligent Fuzzy Sliding Mode Controller for a Bldc Motor." *2017 International Conference on Innovative Mechanisms for Industry Applications (ICIMIA)* (2017). https://doi.org/10.1109/ICIMIA.2017.7975618
[12] Potnuru, D., Mary, K.A., and Babu, C.S. "Experimental Implementation of Flower Pollination Algorithm for Speed Controller of a Bldc Motor." *Ain Shams Engineering Journal* 10, no. 2 (2019): 287-295. https://doi.org/10.1016/j.asej.2018.07.005
[13] Murali, S.B., and Rao, P.M. "Adaptive Sliding Mode Control of Bldc Motor Using Cuckoo Search Algorithm." *2018 2nd International Conference on Inventive Systems and Control (ICISC)* (2018): 989-993. https://doi.org/10.1109/ICISC.2018.8398950
[14] Kommula, B.N., and Venkata, R.K. "Direct Instantaneous Torque Control of Brushless Dc Motor Using Firefly Algorithm Based Fractional Order Pid Controller." *Journal of King Saud University - Engineering Sciences* 32, no. 2 (2020): 133-140. https://doi.org/10.1016/j.jksues.2018.04.007
[15] Khazaee, A., Hosein A.Z., and Gholamreza, A.M. "Loss Model Based Efficiency Optimized Control of Brushless Dc Motor Drive." *ISA Transactions* 86, (2019): 238-48. https://doi.org/10.1016/j.isatra.2018.10.046
[16] Gülbaş, Ö., Hameş, Y., and Furat, M. "Comparison of Pi and Super-Twisting Controller Optimized with Sca and Pso for Speed Control of Bldc Motor." *2020 International Congress on Human-Computer Interaction, Optimization and Robotic Applications (HORA)* (2020): 1-7. https://doi.org/ 10.1109/HORA49412.2020.9152853
[17] Yigit, T., and Hakan, C. "Speed Controlling of the Pem Fuel Cell Powered Bldc Motor with Fopi Optimized by Msa." *International Journal of Hydrogen Energy* 45, no. 60 (2020): 35097-35107. https://doi.org/10.1016/j.ijhydene.2020.04.091
[18] Premkumar, K., and Manikandan, B.V. "Bat Algorithm Optimized Fuzzy Pd Based Speed Controller for Brushless Direct Current Motor." *Engineering Science and Technology, an International Journal* 19, no. 2 (2016): 818-840. https://doi.org/10.1016/j.jestch.2015.11.004
[19] Ibrahim, H.E.A., Hassan, F.N., and Shomer, A.O. "Optimal Pid Control of a Brushless Dc Motor Using Pso and Bf Techniques." *Ain Shams Engineering Journal* 5, no. 2 (2014): 391-398. https://doi.org/10.1016/j.asej.2013.09.013

[20] Wang, X., Siliang, L., Wenping, C., Min, X., Kang, C., Jianming, D., and Shiwu, Z. "Stray Flux-Based Rotation Angle Measurement for Bearing Fault Diagnosis in Variable-Speed Bldc Motors." *IEEE Transactions on Energy Conversion* 36, no. 4 (2021): 3156-3166. https://doi.org/10.1109/TEC.2021.3079444

[21] George, M.A., Dattaguru, V.K., and Thirunavukkarasu, I. "Ota-C Realization of an Optimized Fopid Controller for Bldc Motor Speed Control." *IETE Journal of Research* 69, no. 1 (2023): 118-136. https://doi.org/10.1080/03772063.2021.1951380

[22] Rodríguez-Molina, A., Villarreal-Cervantes, M.G., Serrano-Pérez, O., Solís-Romero, J., and Silva-Ortigoza, R. "Optimal Tuning of the Speed Control for Brushless Dc Motor Based on Chaotic Online Differential Evolution." *Mathematics* 10, no. 12 (2022): 1977. https://doi.org/10.3390/math10121977

[23] Alqarni, Z. "Higher Order Sliding Mode Control for Speed Control of Bldc Motor." *2023 IEEE 13th Annual Computing and Communication Workshop and Conference (CCWC)* (2023): 0212-0217. https://doi.org/10.1109/CCWC57344.2023.10099280